Front. Earth Sci. 2020, 14(1): 37–49
https://doi.org/10.1007/s11707-019-0768-6

RESEARCH ARTICLE

The impact of rapid urban expansion on coastal mangroves: a case study in Guangdong Province, China

Bin AI[1,2,3], Chunlei MA (✉)[1], Jun ZHAO[1,2,3], Rui ZHANG[1]

1 School of Marine Sciences, Sun Yat-Sen University, Guangzhou 510275, China
2 Guangdong Provincial Key Laboratory of Marine Resources and Coastal Engineering, Guangzhou 510275, China
3 Southern Marine Science and Engineering Guangdong Laboratory (Zhuhai), Zhuhai 519000, China

© Higher Education Press and Springer-Verlag GmbH Germany, part of Springer Nature 2019

Abstract Mangroves serve many important ecological functions and consequently represent a dominant coastal ecosystem. However, coastal regions are very susceptible to ecological damage due to their high population density, urban expansion being one of the most important influencing factors. Accordingly, it is vital to ascertain how urban expansion endangers mangrove ecosystems. This study used the decision-tree classification method based on classification and regression tree (CART) algorithm to extract areas of mangrove and built-up land from Landsat images. A correlation analysis was performed between the change in the area of mangroves and the change in the area of built-up land at the cell scale. This study aimed to reveal the magnitude of the influence of urban expansion on mangrove forests in different periods and in different regions, and to identify the places that are seriously affected by urban expansion. The results demonstrate that this approach can be used to quantitatively analyze the impact of urban expansion on mangrove forests, and show that larger areas of mangrove were affected by urban expansion in the past 30 years. The effects of urban expansion were stronger over time, with approximately 12% of cells containing mangroves showing a negative correlation between the increase in the area of built-up land and the change in the area of mangrove forests to different degrees from 2005 to 2015. The same quantitative analysis was also carried out in three subregions of Guangdong Province, namely western Guangdong Province, the Pearl River Delta, and eastern Guangdong Province. It was found that the situations in these three regions were very different due to discrepancies in the distribution of mangroves, the rate of urban expansion, and the awareness of the local government regarding environmental protection. These results can assist in the management of coastal cities and the protection of mangrove ecosystems.

Keywords mangrove, urban expansion, ecological stress, coastal Guangdong

1 Introduction

Mangroves, which include a variety of species, can grow in both tropical and subtropical intertidal zones and can adapt to muddy coastal tidal areas (Bengen, 2001). As a result of the transport of nutrients facilitated by tides, mangrove ecosystems are highly fertile in terms of both land and water; consequently, they are a dominant coastal ecosystem (Gunarto, 2004). Mangrove ecosystems have many important functions, including the protection of biodiversity (FAO, 2007), the reduction of damage caused by storms (BETTS, 2006), and the provision of various economical ecosystem services (Kuenzer et al., 2011). Moreover, approximately 90% of marine animals spend some period of their life cycle in a mangrove ecosystem (Snedaker, 1978). However, as a result of the diverse benefits they present to humans, mangrove ecosystems must withstand high ecological pressures (Yusuf et al., 2017). Due to their high usefulness and vulnerability, mangrove ecosystems have attracted substantial research attention, including studies on the development of classification algorithms, methods to monitor their spatial extents from the local scale to the global scale, and researches into the driving forces behind ecosystem damage (Chandra et al., 2007; Spalding et al., 2010; Kirui et al., 2013; McCarthy et al., 2015; Hamilton and Casey, 2016; Chen et al., 2017).

Surveys of mangrove resources can provide important data for discovering the driving forces that affect mangrove ecosystems. Related reports and researches have indicated that Guangdong Province (GD) has boasted the largest area

Received January 6, 2019; accepted June 27, 2019

E-mail: machl3@mail2.sysu.edu.cn

of mangroves of any province in China for a long time and have proven that, in this region, the area of mangroves and the proportion of the area of mangroves increased between 2000 and 2010. The State Forestry Administration of China reported that in mainland China mangrove ecosystems covered an area of nearly 22000 ha in 2001, and that in 2002, the area of mangrove in GD was about 9084 ha, accounting for almost 41% of China's total (Chen et al., 2009; Spalding et al., 2010). In 2000, the area of mangroves in GD was 7276 ha, accounting for almost 37% of China's total (Spalding et al., 2010). Furthermore, the North-east Institute of Geography and Agroecology and the First Institute of Oceanography reported that, in 2010, the area of mangroves in GD accounted for almost 45% and 49% of China's total, respectively, covering areas of 9289 ha and 12131 ha, respectively (Wu et al., 2013; Jia et al., 2014). However, due to the fact that different methods are used to monitor mangroves, and that different definitions of mangroves are used, the estimated area of mangrove varies greatly, even in the same year. For example, Chen et al. (2017) and Lv et al. (2015) obtained highly discrepant estimates, estimating that, in 2015, the area of mangroves in GD was 8136 ha and 4080 ha, respectively; however, the two studies obtained similar estimates for the proportion of the mangrove area in GD to China's total, reporting values of almost 40% and 45%, respectively. Therefore, it is necessary to use the same means to monitor the variation of mangrove over a long time.

Most existing studies of the areal extent of mangroves have been based on either supervised classification or unsupervised classification methods, which both exhibit poor performance over large areas at different times (Chen et al., 2017). The decision-tree classifier can obtain classification rules directly from training samples, and has the advantage of being independent of the assumptions on value distribution. Unlike many other statistical analysis methods such as maximum likelihood classification, the decision-tree classifier can be independent of variables (Quinlan, 1993; Liu et al., 2008). It is vital to incorporate multi-source ancillary data sets, which usually exhibit different value distributions and are sometimes highly correlated (Jensen, 2005). Therefore in this study, the decision-tree classifier was adopted to retrieve information about the distribution of mangroves.

Meanwhile, in terms of the driving forces that can cause a change in the areal coverage of mangroves, it has been found that mangrove ecosystems have experienced severe erosion worldwide due to both natural and anthropogenic factors; the former category includes climate change, sea surface temperature change, sea level rise, and Spartina invasion (Alongi, 2015; Lu et al., 2018; Ximenes et al., 2018), while the latter category includes deforestation, urban expansion, aquaculture, and agriculture, which erode mangroves either directly (reclamation) or indirectly (pollution and sedimentary accumulation flux in mangrove habitats) (Fan, 1995; Manson et al., 2001; Meng et al., 2016; Estoque et al., 2018). Among these factors, urban expansion is one of the most important, particularly in coastal zones characterized by the rapid development of activities both on land and at sea (Yusuf et al., 2017) which correspondingly result in the increase of population density and in rapid changes in land use types. Most newly constructed built-up land has been gradually converted using reclamation for the construction of buildings and docks (Liu and Liu, 2008; Gao et al., 2014; Wang et al., 2014; Wu et al., 2014; Hou et al., 2016).

Previous research on the driving forces of changes to mangrove ecosystems was almost always conducted from a qualitative perspective. However, it is necessary to discuss the quantitative relationship between such driving forces and changes to mangrove ecosystems. Accordingly, this study used a decision-tree classifier to extract the distribution of mangroves and land use types throughout the coastal regions of GD in 1985, 1995, 2005, and 2015. Then, the level of urban expansion was characterized by analyzing the area of built-up land. This study explores the relationship between urban expansion and the spatial distribution of mangrove ecosystems through correlational analysis methods, and identifies key locations that are beneficial for the development and implementation of mangrove protection policies.

2 Study area and data

This study selected the coastal zone of GD as a sample area. GD, which spans the latitudes from 20°13′ N to 25° 31′ N and the longitudes from 109°39′ E to 117°19′ E, boasts the largest economic aggregate and fastest economic growth among all the provinces in China (Lv et al., 2012). GD has 3368 km of mainland coastline and 1805 km of island coastline; of this, 1288 km is characterized by silty sediment while 498 km is suitable for mangroves (Wu et al., 2011). The annual average temperature and annual average rainfall in GD is 21.9°C and 1790 mm, respectively (Wu et al., 2016). The province has subtropical and tropical monsoon climates, and accordingly experiences a longer flood season than any other province in China and frequently suffers from the effects of rainstorms, tropical cyclones, and strong convection (Wu et al., 2016).

GD can be divided into three regions according to its geographical features: eastern Guangdong (EG), the Pearl River Delta (PRD), and western Guangdong (WG). It was reported that, from 1985 to 2005, a total of 370 km^2 of land reclamation was carried out in the coastal zone and islands of GD, of which 12.6% was in EG, 31.2% in WG, and 56.2% in the PRD, where the areas of built-up land produced by reclamation were 10.94 km^2, 14.76 km^2, and 35.9 km^2, respectively (Gao et al., 2011). Due to the implementation of coastal projects including land reclama-

tion to meet the demand of urban expansion, the area of mangroves in GD fell by 82% between the 1950s and the 1990s, and the community structure and ecological function of mangroves have been significantly degraded (Zhang et al., 2013). It is important to discover the relationship between urban expansion (mainly the expansion of built-up land) and the change in the area of mangroves, which can provide important information for coastal management policies.

When considering the spatial distribution of mangrove ecosystems, many researchers have used buffer zones to delineate potential mangrove sites. For example, a buffer zone with a seaward buffer distance of 10 km was used by Chen et al. (2017) to analyze the eco-environment of the coastal zone, and a similar buffer zone with a landward buffer distance of 10 km was used by Su et al. (2011). Additionally, Kirui et al. (2013) used a similar 10 km buffer zone to map mangroves. To reduce the number of unnecessary calculations, this study only focused on the coastal zone of GD, and a consistent buffer zone, extending 10 km both landward and seaward, was generated for the years 1985, 1995, 2005, and 2015 with the administrative boundaries along the coast of the province and neighboring islands. The research scope and location of the study area are shown in Fig. 1.

In this study, in order to determine the distribution of mangrove forests, eight Landsat images for each year were used, giving a total of 32 images. Images taken between 1985 and 2005 were obtained from Thematic Mapper (TM) scenes collected from Landsat 5, and images taken in 2015 were obtained from Operational Land Imager (OLI) scenes collected from Landsat 8. The spatial resolution of all images was 30 m. The images were downloaded freely from the websites of the Geospatial Data Cloud and the United States Geological Survey (USGS). Due to the difficulty of making direct field observations in mangrove areas, ground truth samples selected from high-resolution images from the Google Earth software were frequently used as field measurements when verifying the accuracy of classification results (Cissell and Steinberg, 2018; Estoque et al., 2018; Han et al., 2018; Jayanthi et al., 2018; Jia et al., 2018; Shrestha et al., 2019). Additionally, high-spatial-resolution images from Google Earth taken in 2015 were also used to verify the classification accuracy. As shown in Table 1, images acquired in 1986 and 1987 were used for the year 1985, and images acquired in 1994–1996, 2004 and 2005, and 2013–2016 were used for the years 1995, 2005, and 2015, respectively, due to the common occurrence of cloudy weather in coastal regions.

3 Methods

The Landsat images used to monitor changes in mangrove areas and built-up land were obtained between 1985 and 2015. The images were preprocessed using methods including radiometric correction, atmospheric correction, geometric correction, seamless mosaic, and image cutting. Then, the preprocessed images were classified to extract areas of mangroves and built-up land using an automatic decision-tree classification method based on the classification and regression tree (CART) algorithm, and the classification results were compared with samples chosen from high-spatial-resolution images. Finally, correlation analysis was performed between the variation in the area of built-up land and that of mangrove forests during two consecutive research years.

3.1 Image preprocessing

First, radiometric corrections were applied to all images to generate exoatmospheric reflection images (Chander

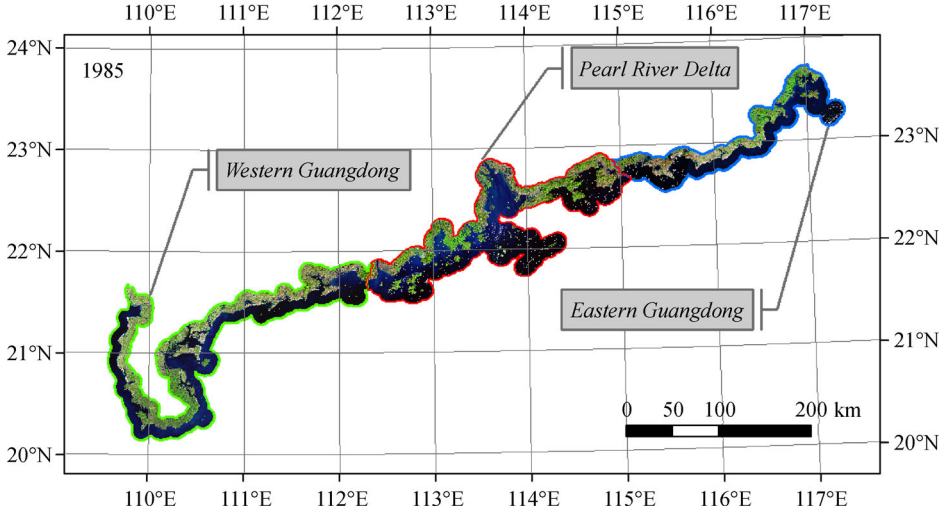

Fig. 1 Cropped image in 1985 of research scope.

Table 1 A list of image datum used in this study

Study year	Number of images	Satellite	Acquisition data	Cloud cover /%	Resolution/m
1985	8	Landsat-5	1986/11/03–1987/12/08	0–9	30
1995	8	Landsat-5	1994/10/22–1996/12/23	0–17	30
2005	8	Landsat-5	2004/11/18–2005/11/23	0–24	30
2015	8	Landsat-8	2013/10/26–2016/09/27	0–17	30

Markham et al., 2009). Then, the Fast Line-of-sight Atmospheric Analysis of Spectral Hypercubes (FLAASH) algorithm was used to implement atmospheric corrections, and geometric corrections were performed on the images from 1985, 1995, and 2015 based on the images acquired in 2005 to ensure that all the images had a similar spatial reference. Then, the Seamless Mosaic tool was used to mosaic the images for each year. During the mosaicking process, the cubic convolution resampling method was used due to its high spatial accuracy (Giri Pengra et al., 2007). Finally, the aforementioned buffer zone was extracted and divided into three parts: EG, the PRD, and WG. Consequently, the study area includes China's Macao and some regions of China's Hong Kong.

3.2 Image classification

Considering the actual situation of GD, six types of land cover were taken into consideration: mangrove, water, farmland, built-up land, other vegetation, and other land use. A decision-tree classifier based on the CART algorithm was used to identify mangrove and built-up land from remote sensing images (Ma et al., 2019). The identification process includes the following main steps:

1) Selecting training samples. As described in previous studies, the false-color composition of Landsat-5 bands 3, 4, and 5 (corresponding to Landsat-8 bands 4, 5, and 6) was deemed to facilitate the detection of mangrove through visual interpretation (Spalding et al., 2010). Therefore, the samples of each land cover type were chosen through the visual interpretation of false-color composites using channels 3, 4, and 5 of the Landsat-5 images and channels 4, 5, and 6 of the Landsat-8 images;

2) Compositing a multi-band image to obtain the features of the training samples. Prior to classification, the normalized difference vegetation index (NDVI) (Tucker, 1979), which is calculated by Eq. (1), and classification results using the iterative self-organizing data analysis technique (ISODATA), were calculated to enhance the separability among samples of different land cover types. Additionally, the inundated mangrove forest index (IMFI) (Jia, 2014), which is expressed by Eq. (2), was calculated to distinguish between flooded mangroves and seawater. Then, the NDVI layer, ISODATA classification result, IMFI layer, and multispectral Landsat bands for each scene were composited into a multi-band image;

3) Analyzing the selected samples and generating classification rules from the composited image via the RuleGen extension tool embedded in ENVI, which can output the decision tree project file automatically.

The spectral characteristics of the same land cover type may vary greatly among different subregions (Li et al., 2015). For example, there was a great disparity in the spectral characteristics of the Landsat images of the vegetation distributed in EG and WG, which would result in misclassification with low accuracies if the uniform classification rules were adopted. To improve the classification accuracy, the samples used to generate the decision tree were individually selected in each subregion, and CART was individually implemented for the images covering EG, the PRD, and WG, rather than being directly implemented for images covering the whole of GD for all the study years (1985, 1995, 2005, and 2015) (Ma et al., 2019), which correspondingly generated a decision-tree project file for each subregion.

$$\mathrm{NDVI} = \frac{R_{\mathrm{nir}} - R_{\mathrm{red}}}{R_{\mathrm{nir}} + R_{\mathrm{red}}}, \tag{1}$$

$$\mathrm{IMFI} = \frac{R_{\mathrm{blue}} + R_{\mathrm{green}} - 2R_{\mathrm{nir}}}{R_{\mathrm{blue}} + R_{\mathrm{green}} + 2R_{\mathrm{nir}}}, \tag{2}$$

where R_{red}, R_{blue}, R_{green}, and R_{nir} represent the reflectance of the red band, blue band, green band, and near-infrared band, respectively.

3.3 Accuracy validation

To measure the quality of the classifications, accuracy measures were used in this study. These were mostly derived on the basis of a comparison of a classification in question with another reference classification that was considered to be reliable and true, and which was often obtained with different methods, e.g., by on-site ground measurements. The confusion matrix, also called a confusion table, can be derived and contains all the information about the relationship between the classification and the reference classification. Then overall accuracy (OA), producer's accuracy (PA), and user's accuracy (UA) can be calculated from the confusion matrix. A detailed introduction to the parameters relating to accuracy validation can be found in Stehman (1997).

OA is defined as the proportion of all reference pixels

which are classified correctly (i.e., for which the class assignments of the classification and the reference classification agree). This can be expressed as follows:

$$P_0 = \frac{\sum_{k=1}^{N} a_{kk}}{\sum_{i,k=1}^{N} a_{ik}} = \frac{1}{n}\sum_{k=1}^{N} a_{kk}, \quad (3)$$

where P_0 is the overall accuracy, N is the total number of reference pixels, a_{ik} is the number of pixels that are classified as the i^{th} type in the classification are just of the k^{th} type in the reference classification, and a_{kk} is the number of pixels that are correctly classified as the k^{th} type in the classification.

PA is an estimate of the probability that a pixel of a certain type in the reference classification is correctly classified. It is thus used to tell how well the classification agrees with the reference classification. The PA for class type i can be expressed as follows:

$$P_i = \frac{a_{ii}}{\sum_{i=1}^{N} a_{ki}}, \quad (4)$$

where P_i is the PA for class type i, a_{ii} is the number of pixels that are correctly classified as the i^{th} type in the classification, and a_{ki} is the number of pixels that are classified as type k in the classification are just of type i in the reference classification.

UA expresses the probability that a pixel classified as a certain type is actually of that type, and is defined as the proportion of pixels for which the classification and the reference classification agree to the total number of reference pixels classified as the same class by the classification method. It can be expressed as follows:

$$U_i = \frac{a_{ii}}{\sum_{i=1}^{N} a_{ik}}, \quad (5)$$

where U_i is the UA for the class type i.

As OA, PA, and UA give no information about what classes are classified with high accuracy, and cannot reflect the agreement of the two classifications for each class, the Kappa coefficient has been widely used to measuring this agreement. It is defined as follows:

$$K = \frac{P_0 - P_e}{1 - P_e}, \quad (6)$$

where can be calculated using the following equation:

$$P_e = \frac{1}{n^2}\sum_{k=1}^{N}\left(\sum_{i=1}^{N} a_{ki} \cdot \sum_{i=1}^{N} a_{ik}\right), \quad (7)$$

where a_{ki} is the number of pixels classified as the k^{th} type in the classification and as the i^{th} type in the reference classification.

Usually, high-spatial-resolution images can be regarded as the ground truth to measure the classification accuracy of mangrove areas. In this study, the classification results were compared with samples chosen from high-spatial-resolution Google Earth images, and the indices OA, Kappa coefficient, UA, and PA were calculated to quantitatively validate the classification accuracy.

3.4 Correlation analysis

With the rapid growth of the urban populations, especially in coastal zones, the amount of built-up land has accordingly and inevitably increased to a large degree to meet the demand for housing, public facilities, and the living environment. This has resulted in the degeneration of ecological spaces such as mangrove ecosystems. Additionally, the degeneration trend of such ecosystems presents different patterns at different degrees of urban expansion. Therefore, the relationship between the extent of urban expansion and the variation in the area of mangroves was further discussed by means of correlation analysis. Therein, the degree of urban expansion was characterized as the variation in the area of built-up land. To establish this relationship, it is necessary to adjust the statistical scale. The regional scale and large grid scale have usually been adopted to perform this adjustment. In this study, considering the relatively scarce distribution of mangroves, the correlation analysis was carried out at the grid scale with a grid side length of 2 km in order to obtain enough grid cells where mangroves existed in each of the four study years. The grid was generated using a fishnet tool embedded in the ArcGIS software. The correlation between the variation in the area of built-up land and that of mangrove forests during two consecutive research years was quantitatively measured within different selected grid cells. Additionally, an iteration procedure was implemented by gradually increasing the area of built-up land from a minimum value to a maximum one. The cells in which the change in the area of built-up land was larger than a defined threshold were extracted. The correlation analysis was terminated when the number of extracted cells was less than 10, and the calculated Pearson correlation coefficients were extracted to represent the influence of urban expansion on mangrove forests. The correlation analysis was performed for the whole of GD and in each of the three regions (EG, the PRD, and WG) to compare the differences among them:

$$\mathrm{Correl}(X,Y) = \frac{\sum (y_i - \overline{y})(y_i^{\wedge} - \overline{y^{\wedge}})}{\sqrt{\sum (y_i - \overline{y})^2 \sum (y_i^{\wedge} - \overline{y^{\wedge}})^2}}, \quad (8)$$

where $y_i^{\wedge}$ is the extent of urban expansion in the sample cell, y_i is the variation in the area of mangrove forests observed for the same cell, and $\overline{y}$ and $\overline{y^{\wedge}}$ are the average extent of

urban expansion and the average variation in the mangrove areas, respectively.

The whole correlation procedure was performed with the use of the ENVI 5.3, ArcGIS 10.3, MATLAB R2016a, GRAPHER 10, and Google Earth software.

4 Results and analysis

4.1 Classification accuracy

During the classification process, the classification results for mangroves and built-up land (including the area and distribution) in the four study years were repeatedly compared with the values obtained in many previous studies or related reports, and manual modification was performed after classification to eliminate the obvious classification errors. Then, accuracy validation was carried out using the four abovementioned quantitative indices (OA, Kappa coefficient, UA, and PA). Since the same method was used to identify mangroves from images collected in all study years, the classification accuracies should be generally similar to each other (Chandra et al., 2007). Due to the difficulty that was associated with acquiring images with a high spatial resolution in previous years, only the accuracy in 2015 was validated. For WG and the PRD, 100 samples were chosen for each land use type, while only 30 samples were selected for the 'other' land use type since it was scarce in the study area. Due to the rarity of mangroves in EG, only 53 mangrove samples were chosen, and the number of samples of the 'other' land type in EG was the same as in WG and the PRD. All samples were randomly chosen and were evenly distributed across the entire study area. The classification accuracies for the three regions in GD for 2015 are shown in Table 2. The overall accuracies were all greater than 90%, and the accuracy for the PRD was greater than those for WG and EG. For the Kappa coefficient, WG had a greater value than the other regions, and all values of Kappa were greater than 0.8. In each of the three regions, the UA and PA of the areas of mangrove and built-up land were greater than 80%. In conclusion, the classification method used herein exhibited an acceptable accuracy, and the subsequent analysis based on the classification results was convincing.

Table 2 Accuracy validation results in 2015

Region	WG	PRD	EG
Overall Accuracy/%	96.08	97.26	93.27
Kappa Coefficient	0.94	0.91	0.89
Producer's Accuracy of mangrove/%	93.01	83.28	80.70
User's Accuracy of mangrove/%	88.41	97.46	89.90
Producer's Accuracy of building land/%	99.47	98.57	98.99
User's Accuracy of building land/%	88.55	80.68	91.84

4.2 Values of correlation coefficients

To perform the correlation analysis to discover the influence of the spread of built-up land on mangroves, a total of 1900 cells with a side length of 2 km were extracted. As mentioned above, in order to eliminate irrelevant cells, iterations were performed to select different thresholds for the change in the area of built-up land. Accordingly, Pearson correlation coefficients and their P-values were calculated based on those different thresholds. As the thresholds increased, the correlations between the change in the area of built-up land and the change in the area of mangrove became increasingly negative. In this way, a table of Pearson correlation coefficients was obtained. The Pearson correlation coefficients were iterated from the first value to the last value to determine which cells had different values, and the cells with Pearson correlation coefficients of approximately -0.3, -0.5, -0.6, and -0.7 were extracted for further analysis. If the Pearson correlation coefficient was greater than -0.3, there was no strong negative correlation between the change in the area of built-up land and the change in the area of mangroves; if the Pearson correlation coefficient was less than -0.3 and greater than -0.5, there was a moderate negative correlation between them; and, if the Pearson correlation coefficient was less than -0.5, there was a strong negative correlation between them. The smallest Pearson correlation coefficients for GD, WG, the PRD, and EG were approximately -0.23, -0.12, -0.19, and -0.44, respectively, from 1985 to 1995, -0.65, -0.74, -0.65, and -0.07, respectively, from 1995 to 2005, and -0.77, -0.74, -0.40, and -0.22, respectively, from 2005 to 2015. In the period from 1985 to 1995, only EG showed a moderate negative correlation between the change in the area of built-up land and the change in the area of mangroves. In the period from 1995 to 2005, all regions except EG showed strong negative correlations. In the period from 2005 to 2015, GD showed a strong negative correlation of -0.77, and WG also showed a strong negative correlation. The PRD showed only a moderate negative correlation, while EG showed no strong negative correlation. The P-values are shown in Table 3; most of them are less than 0.05, indicating that the majority of correlations were significant.

4.3 The spatiotemporal distribution of mangroves and built-up land

The total areas of mangrove forest during the period from 1985 to 2015 are shown in Fig. 2. The total area of mangroves in GD experienced a net increase of 395 ha during the past 30 years. During the period from 1985 to 1995, the area of mangroves showed a slight increase of nearly 250 ha, almost all of which was located in WG, mainly scattered in Zhanjiang, Suixi, and Lianjiang cities (Ma et al., 2019). However, a sharp decrease in the area of

Table 3 Correlation coefficients calculated in GD, WG, PRD, EG

Region	$-0.5 < r \leqslant -0.3$			$-0.6 < r \leqslant -0.5$		
	1985–1995	1995–2005	2005–2015	1985–1995	1995–2005	2005–2015
GD	——	0.1625	1.28E-06	——	0.0268	4.78E-06
EG	0.0010	——	——	——	——	——
PRD	——	0.1625	5.19E-05	——	0.0268	——
WG	——	0.0038	2.12E-05	——	0.0038	0.0019
Region	$-0.7 < r \leqslant -0.6$			$-0.8 < r \leqslant -0.7$		
	1985–1995	1995–2005	2005–2015	1985–1995	1995–2005	2005–2015
GD	——	0.0248	0.0032	——	——	0.0061
EG	——	——	——	——	——	——
PRD	——	0.0248	——	——	——	——
WG	——	0.0038	0.0009	——	0.0038	0.0017

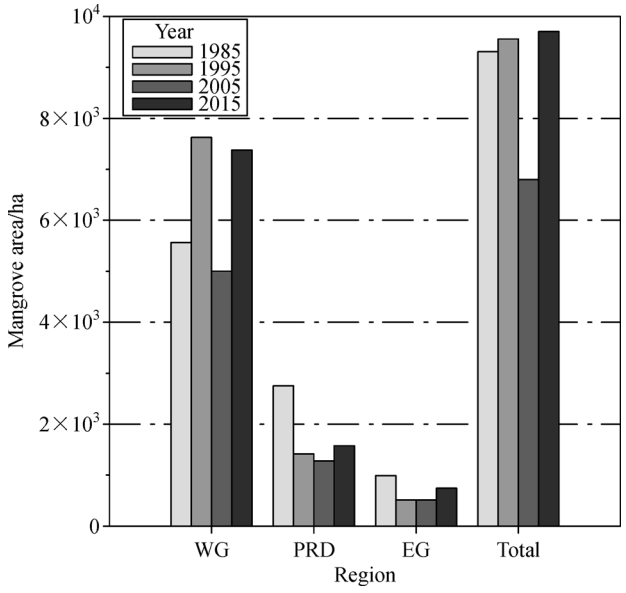

Fig. 2 Total area of mangroves in GD during the period from 1985 to 2015.

mangroves occurred in the period from 1995 to 2005, leaving only 6793 ha remaining. From 2005 to 2015, an increase in mangrove area was observed for all subregions, with the largest growth in area being observed in Leizhou, Lianjiang, and Zhuhai cities. The increase in the area of mangrove forests in WG detected in the present study is similar to that reported by (Jia et al., 2018). Remarkably, in 2015, the area of mangrove increased to 9700 ha. The tendency of mangrove growth observed for WG was similar to that observed throughout GD, except that in WG a sharp increase was observed from 1985 to 1995, with a net increase of 1816 ha over the past 30 years. Net decreases of 1173 ha and 248 ha over the past 30 years were detected in the PRD and EG, respectively. In the PRD, the area of mangroves sharply decreased from 1985 to 1995, slightly decreased from 1995 to 2005, and increased from 2005 to 2015. In EG, the area of mangroves showed a decrease from 1985 to 1995 and an increase from 2005 to 2015, with the area in 1995 being similar to that in 2005. Most mangroves in GD were located in WG, which contained 59.79%, 79.84%, 73.67%, and 76.07% of the total area of mangroves in GD in 1985, 1995, 2005, and 2015, respectively. Meanwhile, EG contributed the least, only containing 10.63%, 5.38%, 7.54%, and 7.64% of the total area of mangroves in GD in 1985, 1995, 2005, and 2015, respectively.

The spatial distribution of built-up land was also retrieved from the classification results. The total areas of built-up land are shown in Fig. 3. The area of built-up land in GD showed a continuously increasing tendency over the

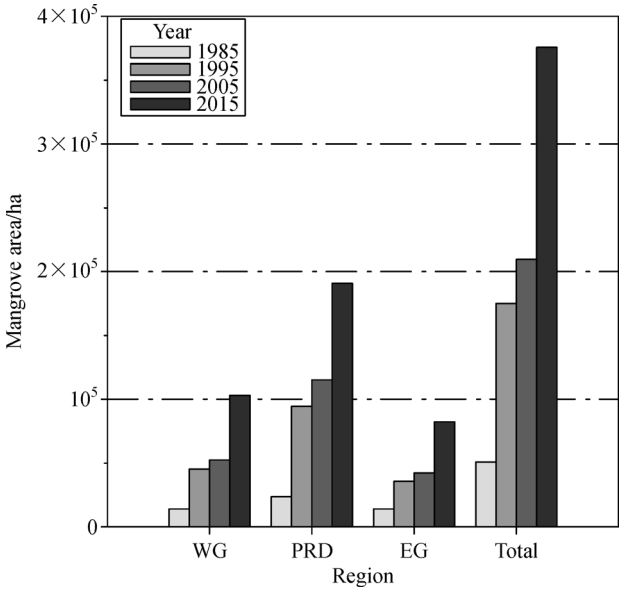

Fig. 3 Distribution of built-up land in GD in 1985, 1995, 2005, and 2015.

past 30 years. From 1985 to 1995 and from 2005 to 2015, sharp increases of 124350 ha and 166283 ha, respectively, were observed in the area of built-up land. The three regions (WG, the PRD, and EG) showed tendencies that were similar to the whole of GD. The annual growth rates in the area of built-up land in WG, the PRD, and EG from 1985 to 1995 were 23.37%, 30.24%, and 16.10%, respectively, while the annual growth rates from 2005 to 2015 in WG, the PRD, and EG were 9.69%, 6.58%, and 9.57%, respectively. In the period from 1985 to 1995, the greatest annual growth rate was observed in the PRD. In WG, built-up land expanded quickly in Zhanjiang, and expanded slowly in Suixi and Lianjiang. In the period from 2005 to 2015, WG exhibited the greatest annual growth rate in the area of built-up land, namely 9.69%, which was slightly greater than that of EG; although the expansion of built-up land in Leizhou and Lianjiang was slower than in other cities in the same period, the expansion was still fast. In the PRD, built-up land expanded rapidly in Shenzhen and Zhuhai during the period from 2005 to 2015. The PRD had the largest area of built-up land in each of the study years, and the areas of built-up land in WG were similar to those in EG in all study years.

By comparing the variation in the areas of mangroves and built-up land, it can be seen that although there was an increase in the area of mangrove with the expansion of built-up land due to the influence of both natural and anthropogenic factors, the rapid expansion of built-up land resulted in an overall decrease in the total area of mangroves over the past three decades. This will be further discussed in the following sections.

4.4 Correlation pattern

Both the spatial distribution and the overall variation of mangrove forests and built-up areas show strongly periodic differences among different subregions in the coastal zone of GD. The influences of urban expansion on mangrove forests in EG, the PRD, and WG were highly dissimilar to one another. Therefore, the variation trend of the correlation between the change in the area of mangrove forests and the increase in the area of built-up land was also calculated and discussed for each subregion in this study.

4.4.1 Guangdong Province

As shown in Fig. 4, in the period from 1985 to 1995, no cells showed a negative correlation between the increase in the area of built-up land and the change in the area of mangrove forests in the entire GD. However, from 1995 to 2005, some cells began to show moderate and strong negative correlations. Moreover, from 2005 to 2015, approximately 12% of cells showed negative correlations to different degrees. In GD, an increasing number of cells were seriously affected by urban expansion in the past 30 years, and the effects became stronger over time. From 1995 to 2005, in the cells with r values between -0.3 and -0.5, between -0.5 and -0.6, and between -0.6 and -0.7, there were net losses of mangrove areas of approximately 6.36, 3.6, and 3.6 ha, respectively. From 2005 to 2015, in the cells with r values between -0.3 and -0.5, between -0.5 and -0.6, between -0.6 and -0.7, and less than -0.7, there were net losses of mangrove

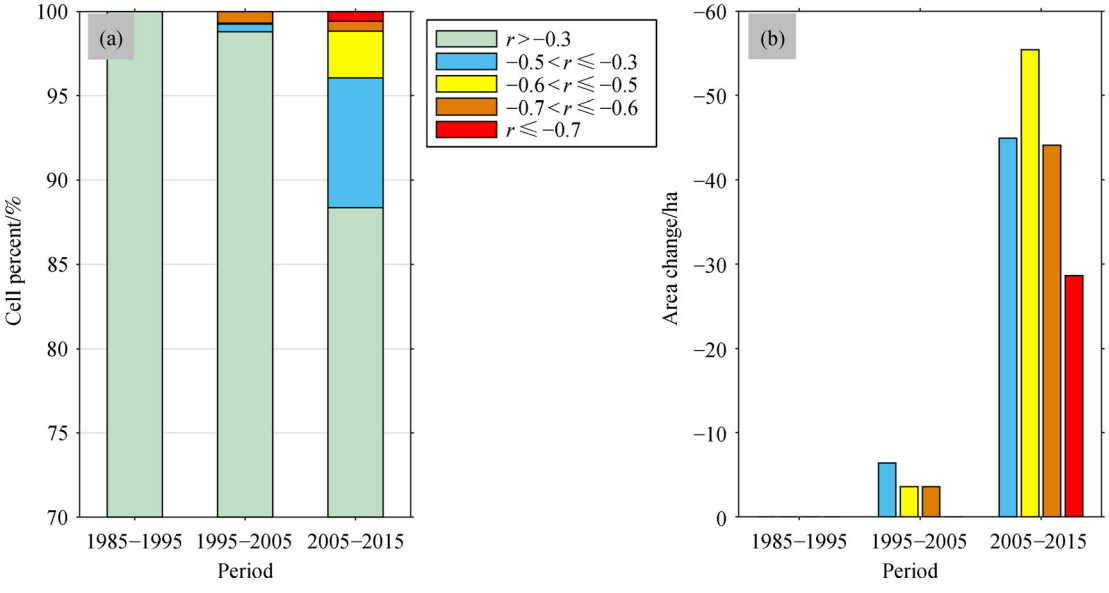

Fig. 4 Proportion of different r values in GD (a) and the mangrove areas change in cells of different r in GD (b).

areas of approximately 44.98, 55.42, 44.14, and 28.62 ha, respectively. The cells with a strong negative correlation between the increase in the area of built-up land and the change in the area of mangrove forests can be found to help protect mangroves from the influence of urban expansion. The r values from 2005 to 2015 are mapped in Fig. 5, which shows that a strong negative correlation always occurs around cities due to urban expansion, industrial development, port construction, etc. (subgraphs A, B, D, and E), and the absolute values of r are relatively low in natural reserves, such as Qi'ao Island (subgraph C).

4.4.2 Eastern Guangdong

There is a relatively small area of mangrove forest in EG. In this region, the increase in the area of built-up land typically changed periodically. Additionally, most of the mangrove forests in EG are located far away from built-up areas. The mangrove forests in this region have been relatively less affected by urban expansion. As shown in Fig. 6, a moderate negative correlation was observed between the increase in the area of built-up land and the change in the area of mangrove forests in only approximately 25% of the cells in EG during the period from 1985 to 1995, while only a weak negative correlation was observed from 1995 to 2005. Furthermore, of the cells where mangrove forests were distributed, approximately 12% were affected by urban expansion, with r values between -0.3 and -0.5. In conclusion, urban expansion only affected mangroves in EG from 1985 to 1995, and the effect was weak. This may be due to the scarcity of mangroves and the slower speed of urban expansion in EG.

4.4.3 Pearl River Delta

As shown in Fig. 7, from 1985 to 1995, no cells in the PRD showed a negative correlation between the increase in the area of built-up land and the change in the area of mangrove forests. However, from 1995 to 2005, some cells began to show moderate and strong negative correlations. Moreover, from 2005 to 2015, approximately 14% of the cells showed a negative correlation with different magnitudes. In the PRD, an increasing number of cells have been affected by urban expansion over the past 30 years, however the effects were weaker during the past 20 years. In 2005 and 2015, approximately 5% of mangrove forests

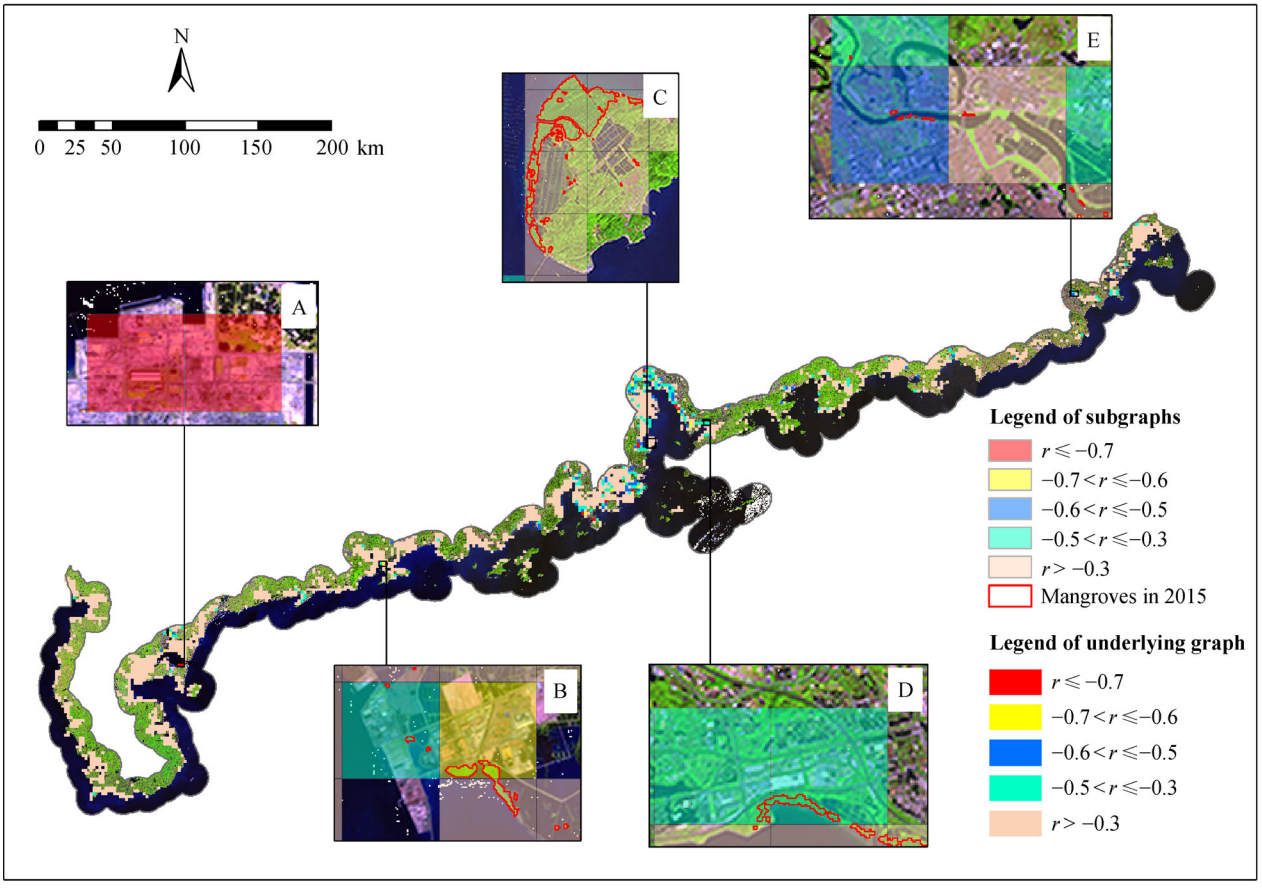

Fig. 5 Spatial pattern of different r values from 2005 to 2015 in GD. The polygons with red outlines in subgraphs show the position of mangroves in 2015.

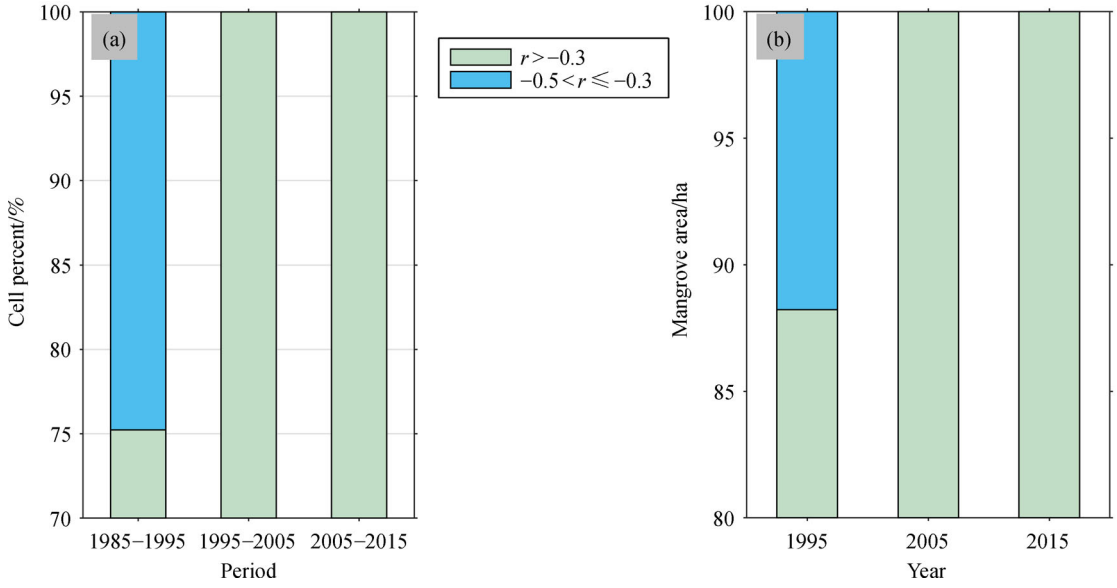

Fig. 6 Proportion of different r values in EG (a) and proportion of mangrove areas in cells of different r values in EG (b).

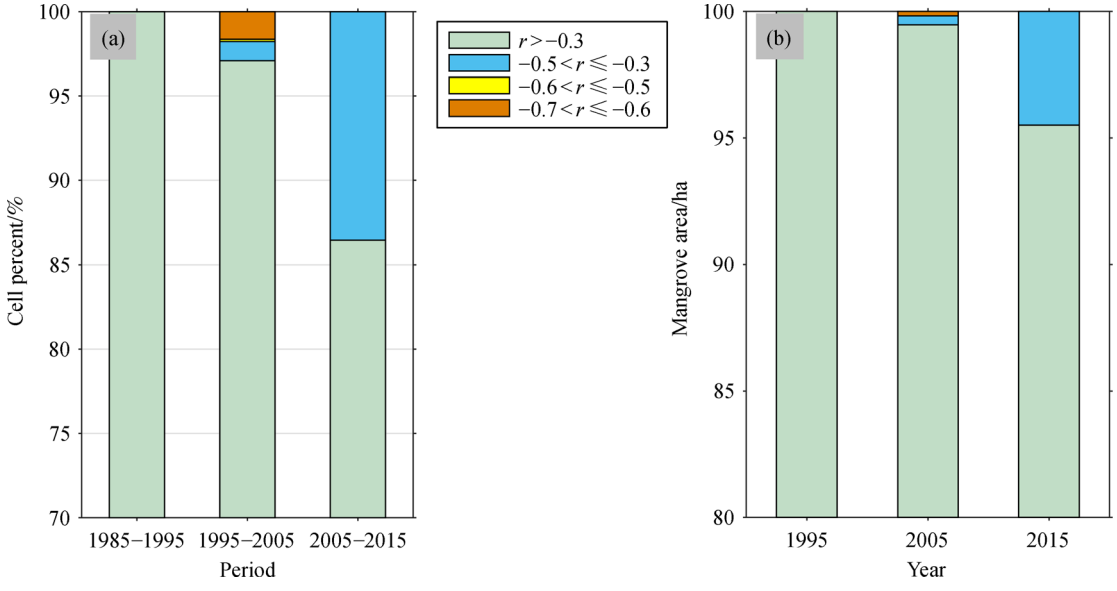

Fig. 7 Proportion of different r values in PRD (a) and proportion of mangrove areas in cells of different r values in PRD (b).

were affected by the increase in the area of built-up land, with r values between -0.3 and -0.5. Although a substantial proportion of the cells in the PRD were affected by urban expansion, a relatively small amount of the total mangrove area was affected by the rapid increase in the area of built-up land.

4.4.4 Western Guangdong

As shown in Fig. 8, from 1985 to 1995, no cells in WG showed a negative correlation between the increase in the area of built-up land and the change in the area of mangrove forests. However, from 1995 to 2005, some cells began to show moderate and strong negative correlations. Moreover, from 2005 to 2015, approximately 24% of the cells showed a negative correlation with different magnitudes. In WG, an increasing number of cells have been affected by the expansion of built-up land over the past 30 years, and the effects were stronger than those in the PRD. During the period from 2005 to 2015, approximately 9%, 0.5%, and 0.3% of all mangroves were affected by urban expansion, with r values from -0.3 to -0.5, from -0.6 to

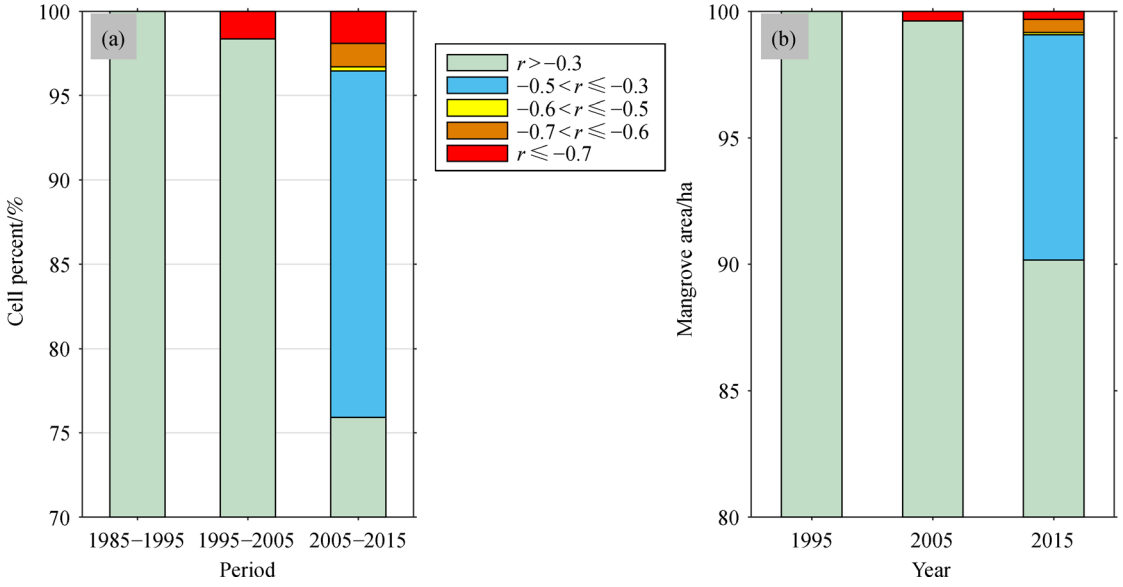

Fig. 8 Proportion of different r values in WG (a) and proportion of mangrove areas in cells of different r values in WG (b).

−0.7, and less than −0.7, respectively. From 2005 to 2015, both the proportion of cells affected by urban expansion and the area of mangroves affected by urban expansion were large in WG.

5 Discussion

This study developed an analytical framework to quantitatively determine the relationship between the expansion of built-up land and the distribution of mangroves at the cell scale. This method was applied to the coastal zone of GD from 1985 to 2015. The cells in which urban expansion had a large negative impact on the area of mangrove forests were able to be correctly identified using this framework. Although the optimal cell size remains to be confirmed, cells with a side length of 2 km proved to be feasible in this study; however, whether this scale could be applied to other regions is still uncertain. Considering the large area and the long time period analyzed in this study, the areas of mangroves and built-up land were classified from Landsat images with moderate spatial resolution, which are freely available and have been frequently used in previous studies. As a result, patches of mangrove which are smaller than the spatial resolution of the images cannot be monitored, and some areas of mudflat or aquaculture may be misclassified as mangroves due to the existence of mixed pixels; thus, the accuracy of classification was inevitably affected. It is worth developing methods for the decomposition of mixed pixels to distinguish other land use types from mangroves over small areas. Images with a higher spatial resolution would be preferable when the study area is small, since they can provide more information about the density, biodiversity, and community structure of mangrove ecosystems, as well as the area of mangroves. This can help to inform discussions of ecological stress on mangrove ecosystems caused by rapid urban expansion.

The relationship analysis indicated that the correlation patterns for GD, EG, PRD, and WG were significantly different. This was determined by not only the discrepancies in the estimated mangrove distribution area and the rate of urban expansion, but also the awareness of mangrove protection. In EG, the expansion of built-up land had relatively little influence on mangroves, since mangroves are scarce in this region and most of them are far from built-up land. In the PRD, several Mangrove Natural Reserves have been set up, with the aim of protecting mangroves from erosion caused by the rapid expansion of built-up land. In WG, mangroves are widely distributed, and therefore when built-up land started to be rapidly expanded in the coastal zone, it was difficult to avoid this development from affecting mangroves, although the awareness of mangrove conservation has been enhanced over time. Furthermore, the spatiotemporal variation in the area of mangrove forests is also influenced by the patterns and types of urban expansion, which may lead to the distance-decay effect. It is necessary to further discuss this issue in future studies.

6 Conclusions

In this study, quantitative analysis was carried out to determine the impact of rapid urban expansion on mangrove forests. The spatial distribution of mangrove forests and built-up land was first obtained from multitemporal remote sensing images. It can be concluded that the total area of mangrove forests experienced a net increase over the past 30 years in the coastal zone of

Guangdong Province. The majority of mangroves in Guangdong Province were located in western Guangdong, while eastern Guangdong contained the lowest area of mangroves of all the subregions of the province. The total amount of built-up land in Guangdong Province has continuously increased over the past 30 years. The expansion of built-up land in the three subregions of Guangdong Province was similar to that observed in the whole province. Over the past 30 years, the total area of mangrove forest and built-up land presented periodic variation and also varied according to the region.

With the increase in the amount of built-up land, an increasing number of mangrove forests have been affected by urban expansion over the past 30 years, and the effects have grown stronger over time. However, the influence of the expansion of built-up land on mangrove forests differed greatly among the subregions. Urban expansion affected mangroves in EG only from 1985 to 1995, and the effect was weak. This may be due to the scarcity of mangroves and the slower speed of the urban expansion in this region. Similarly, in the PRD, an increasing number of mangrove forests have been affected by urban expansion over the past 30 years, although the effects were weaker during the past 20 years. Additionally, in WG, an increasing number of mangrove forests have also been affected by urban expansion, and the effects were relatively strong. This study indicates that a strong negative correlation between the increase in the area of built-up land and the change in the area of mangrove forests always existed around cities, and the absolute values of r were low in natural reserve areas.

According to the analysis of the influence of urban expansion on the variation of mangrove forests, areas with a strong negative correlation were detected. This could help to determine how to protect mangroves from the influence of urban expansion. The fact that dissimilar correlation patterns were observed in the three subregions of Guangdong Province requires the establishment of a partitioned mangrove protection mechanism. For instance, in EG, a larger area of mangroves can be planted artificially in tidal flats, which are suitable for mangrove growth, and more mangrove reserves can be established. In the PRD, where the expansion of built-up land will be relatively stable, urban expansion will continue to influence mangroves, and more frequent monitoring of mangroves is therefore required. In WG, the expansion of built-up land in the landward direction, rather than the seaward direction, is recommended. In the whole of Guangdong Province, it is important to draw an ecological red line for restraining urban growth and carry out regular monitoring, strict supervision of ecological protecting, and enforcement of relevant regulations for the purpose of the ecological protection of mangroves.

Acknowledgements The authors would like to thank the anonymous reviewers for their suggestions and comments. This research was supported by the National Natural Science Foundation of China (Grant No. 41301418), the Natural Science Foundation of Guangdong Province (Grant No. 2014A030313141), and the Science and Technology Plan Project of Guangzhou City (Grant No. 201607020041).

References

Alongi D M (2015). The impact of climate change on Mangrove Forests. Curr Clim Change Rep, 1(1): 30–39

Bengen D G (2001). Coastal and marine ecosystems and natural resources: synopsis. Institute of Coastal and Ocean Resources Institute. Bogor Agriculture

BETTS T (2006). An assessment of mangrove cover and forest structure in Las Perlas, Panama. Dissertation for Master's Degree. Edinburgh: Heriot-Watt University

Chander G, Markham B L, Helder D L (2009). Summary of current radiometric calibration coefficients for Landsat MSS, TM, ETM +, and EO-1 ALI sensors. Remote Sens Environ, 113(5): 893–903

Chandra G, Zhu Z, Tieszen L, Singh A, Gillette S, Kelmelis J A (2007). Mangrove forest distributions and dynamics (1975–2005) of the tsunami-affected region of Asia. J Biogeogr, 35: 519–528

Chen B, Xiao X, Li X, Pan L, Doughty R, Ma J, Dong J, Qin Y, Zhao B, Wu Z, Sun R, Lan G, Xie G, Clinton N, Giri C (2017). A mangrove forest map of China in 2015: analysis of time series Landsat 7/8 and Sentinel-1A imagery in Google Earth Engine cloud computing platform. ISPRS J Photogramm Remote Sens, 131: 104–120

Chen L, Wang W, Zhang Y, Lin G (2009). Recent progresses in mangrove conservation, restoration and research in China. J Plant Ecol, 2(2): 45–54

Cissell J R, Steinberg M K (2019). Mapping forty years of mangrove cover trends and their implications for flats fisheries in Cinaga de Zapata, Cuba. Environ Biol Fishes, 102(2): 417–427

Estoque R, Myint S W, Wang C, Ishtiaque A, Aung T T, Emerton L, Ooba M, Hijioka Y, Mon M S, Wang Z, Fan C (2018). Assessing environmental impacts and change in Myanmar's mangrove ecosystem service value due to deforestation (2000–2014). Glob Change Biol, 24(11): 5391–5410

Fan H Q (1995). Mangrove resources, human disturbance and rehabilitation action in China. Chin Biodiv, 3(Suppl.): 49–54

FAO (2007). The world's mangroves 1980-2005. A thematic study prepared in the framework of the global forest resources assessment 2005. Forest Economics and Policy Div Fon

Gao Y, Su F Z, Sun X Y, Yang X M, XUE Z S, Zhang D D (2011). A study on driving forces of land use change of Guangdong Province coastal zone and islands in recent 20a. Acta Oceanol Sin, 33(4): 95–103

Gao Z, Liu X, Ning J, Lu Q (2014). Analysis on changes in coastline and reclamation area and its causes based on 30-year satellite data in China. Transactions of the Chinese Society of Agricultural Engineering, 30: 140–147 (in Chinese)

Giri C, Pengra B, Zhu Z, Singh A, Tieszen L L (2007). Monitoring mangrove forest dynamics of the Sundarbans in Bangladesh and India using multi-temporal satellite data from 1973 to 2000. Estuar Coast Shelf Sci, 73(1-2): 91–100

Gunarto (2004). Mangrove conservation as a supporter of coastal fishery biological resources. Agricultural Research and Development

Journal, 23(1): 15–21

Hamilton S E, Casey D (2016). Creation of a high spatio-temporal resolution global database of continuous mangrove forest cover for the 21st century (CGMFC-21). Glob Ecol Biogeogr, 25(6): 729–738

Han X, Feng L, Hu C, Kramer P (2018). Hurricane influenced changes in the Everglades National Park mangrove forest: Landsat observations between 1985 and 2017. J Geophys Res Biogeosci, 123(11): 3470–3488

Hou X, Wu T, Hou W, Chen Q, Wang Y, Yu L (2016). Characteristics of coastline changes in mainland China since the early 1940s. Sci China Earth Sci, 59(9): 1791–1802

Jayanthi M, Thirumurthy S, Nagaraj G, Muralidhar M, Ravichandran P (2018). Spatial and temporal changes in mangrove cover across the protected and unprotected forests of India. Estuar Coast Shelf Sci, 213: 81–91

Jensen J R (2005). Introductory Digital Image Processing: A Remote Sensing Perspective. 3rd ed. NJ, USA, Upper Saddle River, Prentice Hall, Inc

Jia M (2014). Remote Sensing analysis of China's mangrove forests dynamics during 1973 to 2013. Dissertation for the Doctoral Degree. Beijing: Chinese Academy of Sciences

Jia M, Wang Z, Li L, Song K, Ren C, Liu B, Mao D (2014). Mapping China's mangroves based on an object-oriented classification of Landsat imagery. Wetlands, 34(2): 277–283

Jia M, Wang Z, Zhang Y, Mao D, Wang C (2018). Monitoring loss and recovery of mangrove forests during 42 years: the achievements of mangrove conservation in China. Int J Appl Earth Obs Geoinf, 73: 535–545

Kirui K B, Kairo J G, Bosire J, Viergever K M, Rudra S, Huxham M, Briers R A (2013). Mapping of mangrove forest land cover change along the Kenya coastline using Landsat imagery. Ocean Coast Manage, 83: 19–24

Kuenzer C, Bluemel A, Gebhardt S, Vo T, Dech S (2011). Remote sensing of mangrove ecosystems: a review. Remote Sens, 3(5): 878–928

Li F, Liang H, Mi X, Wei A (2015). A multi-subregions decision tree land cover classification approach using Landsat8 image. Infrared and Laser Engineering, 44(7): 2224–2230

Liu K, Li X, Shi X, Wang S (2008). Monitoring mangrove forest changes using remote sensing and GIS data with decision-tree learning. Wetlands, 28(2): 336–346

Liu W, Liu B Q (2008). Current situation and countermeasures of sea reclamation in China. Guangzhou Env Sci, 23: 26–30

Lu C, Liu J, Jia M, Liu M, Man W, Fu W, Zhong L, Lin X, Su Y, Gao Y (2018). Dynamic analysis of mangrove forests based on an optimal segmentation scale model and multi-seasonal images in Quanzhou Bay, China. Remote Sens, 10(12): 2020

Lv L, Luo H, Zhang B (2012). Relationship between electricity consumption and economic growth of Guangdong Province in China. Front Energy, 6(4): 351–355

Lv T, Zhou X, Liu C, Tao Z,Yongyut T (2015). Spatial distribution dataset of mangrove forests in South Asia (Mangrov_SEAsia_2015). Global Change Research Data Publishing and Repository

Ma C, Ai B, Zhao J, Xu X, Huang W (2019). Change Detection of Mangrove Forests in Coastal Guangdong during the Past Three Decades Based on Remote Sensing Data. Remote Sens, 11(8): 921

Manson F J, Loneragan N R, McLeod I M, Kenyon R A (2001). Assessing techniques for estimating the extent of mangroves: topographic maps, aerial photographs and Landsat TM images. Mar Freshw Res, 52(5): 787–792

McCarthy M J, Merton E J, Muller-Karger F E (2015). Improved coastal wetland mapping using very-high 2-meter spatial resolution imagery. Int J Appl Earth Obs Geoinf, 40: 11–18

Meng X, Xia P, Li Z, Meng D (2016). Mangrove degradation and response to anthropogenic disturbance in the Maowei Sea (SW China) since 1926 AD: Mangrove-derived OM and pollen. Org Geochem, 98: 166–175

Quinlan J R (1993). C4.5 Programs for Machine Learning. San Mateo, USA, Morgan Kaufmann Publishers, Inc

Shrestha S, Miranda I, Kumar A, Pardo M L E, Dahal S, Rashid T, Remillard C, Mishra D R (2019). Identifying and forecasting potential biophysical risk areas within a tropical mangrove ecosystem using multi-sensor data. Int J Appl Earth Obs Geoinf, 74: 281–294

Snedaker S C (1978). Mangrove: Their value and perpetuation. Nat Resour, 14: 6–13

Spalding M, Kainuma M, Collins L (2010). World Atlas of Mangroves. Routledge

Stehman S V (1997). Selecting and interpreting measures of thematic classification accuracy. Remote Sens Environ, 62(1): 77–89

Su P, Guo Z, Xie M, Ye S, Wang D (2011). Analyzing the changes of landscape pattern in the coastal zone based on GIS and RS: a case study of Nantong, China. In: 2011 International Conference on Remote Sensing, Environment and Transportation Engineering. IEEE: 2932–2936

Tucker C J (1979). Red and photographic infrared linear combinations for monitoring vegetation. Remote Sens Environ, 8(2): 127–150

Wang W, Liu H, Li Y, Su J (2014). Development and management of land reclamation in China. Ocean Coast Manage, 102: 415–425

Wu H Y, Liu W Q, Zhang J, Li C M (2016). Summary of the Climate of Guangdong Province in 2015. Guangdong Meteorology, 38: 1–5

Wu P, Ma Y, L X M, Yu G H (2011). Remote sensing monitoring of the mangrove forests resources of Guangdong Province. J Mar Sci, 29: 16–24

Wu P Q, Zhang J, Ma Y, Li X M (2013). Remote sensing monitoring and analysis of the changes of mangrove resource in China in the past 20 years. Adv Mar Sci, 31: 406–414

Wu T, Hou X, Xu X (2014). Spatio-temporal characteristics of the mainland coastline utilization degree over the last 70 years in China. Ocean Coast Manage, 98: 150–157

Ximenes C A, Ponsoni L, Lira F C, Koedam N, Dahdouh-Guebas F (2018). Does Sea Surface Temperature Contribute to Determining Range Limits and Expansion of Mangroves in Eastern South America (Brazil)? Remote Sens, 10(11): 1787–1798

Yusuf D N, Prasetyo L B, Kusmana C, Machfud (2017). Geospatial approach in determining anthropogenic factors contributed to deforestation of mangrove: a case study in Konawe Selatan, Southeast Sulawesi. In: IOP Conference Series: Earth and Environmental Science, 54(1): 012049

Zhang C, Xie J, Lou Q, Zhuang D (2013). Study on experience and countermeasures of fill up sea and build land in Guangdong. Marine Environmental Science, 32(2): 311–315